JOURNAL OF OPTOELECTRONICS AND ADVANCED MATERIALS Vol. 8, No. 6, December 2006, p. 1989 - 1995

Heterojunctions of hydrogenated amorphous silicon and monocrystalline silicon

W. FUHS*, L. KORTE, M. SCHMIDT
Hahn-Meitner-Institut Berlin Kekuléstr.5, D-12489 Berlin, Germany

Heterojunctions of hydrogenated amorphous silicon and monocrystalline silicon, a-Si:H/c-Si, are of technological interest in particular for highly efficient solar cells. Here, we report about studies of the most important material and device parameters of such pn- and np- heterojunctions and their performance as solar cells and light emitting diodes. The electronic structure of the heterojunction is characterized by unsymmetrical band offsets at the conduction and valence bands, ΔE_C and ΔE_V, of 0.14 eV and 0.45 eV, respectively. It is shown that the performance of the devices is strongly determined by the defect structure of the thin doped amorphous emitter layer and the density of states at the amorphous/crystalline interface. This work led to confirmed solar cell efficiencies of 19.8 % for a textured a-Si:H(p)/c-Si(n)/a-Si:H(n) structure without using undoped a-Si:H(i) buffer layers. Heterojunction solar cells are shown to exhibit electroluminescence of high power efficiency (0.3 %) under forward bias.

(Received October 10, 2006; accepted November 2, 2006)

Keywords: Amorphous silicon, Heterojunctions, Band-offset, Solar cells, Light emitting diodes

1. Introduction

The investigation of heterojunctions between amorphous and crystalline semiconductors dates back to the early days of research in the field of amorphous semiconductors. In fact, the first studies have been performed by the Bucharest group on junctions between amorphous and monocrystalline Ge and Si in 1964 [1, 2]. In this early work of Grigorovici *et al.*, the amorphous films were prepared by thermal evaporation without hydrogenation. Therefore, the device performance was determined by the high defect density of the amorphous films and inefficient passivation of the a-Si/c-Si interface. In the early seventies the plasma deposition technique (PECVD) came into use where silane is decomposed in a high frequency glow discharge [3]. This method led to amorphous silicon films of much lower defect density [4] which, as it turned out later, was due to the beneficial role of incorporated hydrogen which saturated Si-dangling bonds and allowed the growth of a more relaxed amorphous network. In 1974 heterojunctions of PECVD-deposited undoped hydrogenated amorphous silicon, a-Si:H, with monocrystalline silicon were studied by Fuhs *et al.* [5]. From a study of the spectral dependence of the photovoltage it was concluded that the p-type Si crystal was depleted at the interface with a built-in potential of 0.3 eV. In addition, a depletion region for electrons was created in the undoped n-type a-Si:H film at the top molybdenum contact. In the late eighties Sanyo Corporation developed a-Si:H/c-Si heterojunctions for application as solar cells. The first studies using n-type c-Si as substrate and a thin boron doped a-Si:H(p) emitter led to efficiencies close to 12 % [6]. Later, Sanyo reported laboratory efficiencies of above 21 % using a more sophisticated device structure (HIT-cells) which involved thin buffer layers of undoped a-Si:H [7]. Meanwhile, Sanyo has started the production of commercial photovoltaic HIT-modules. Certainly the inherent advantage of the plasma technology to passivate the amorphous/crystalline silicon interface effectively by hydrogen was a key for this successful development. For quite a while this approach was almost entirely pursued in Japan as a low-cost high-efficiency route for wafer based solar cells. In the last years many European groups have started work in this direction [8], which involved both research into the physical properties of the heterojunction and the development of devices. Laboratory efficiencies have been reported of up to 19.8 % [9], and it was demonstrated that such heterojunctions have also interesting properties as efficient Si-based light emitting diodes [10].

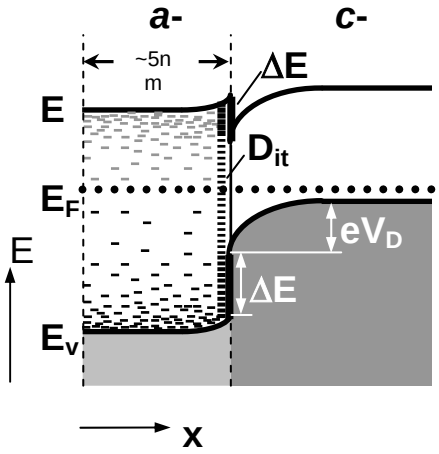

Fig. 1. Schematic band diagram of the amorphous-crystalline heterojunction, drawn for the case of a slightly n-type a-Si:H layer on p-type c-Si substrate. Marked are the band edges E_V, E_C, the band offsets ΔE_V, ΔE_C and the built-in potential eV_D. The dashes in the a-Si:H band gap denote the localized gap states, D_{it} is the density of a-Si:H/c-Si interface states.

At 300 K the optical band gap of the a-Si:H films is about 1.75 eV as defined from a Tauc plot of the optical absorption data, $(\alpha\hbar\omega)^{1/2}$ vs (E_V - $\hbar\omega$), whereas the band gap of crystalline silicon amounts to 1.15 eV. The different width of the band gaps causes band offsets at the conduction and valence bands, ΔE_C and ΔE_V, which are very important intrinsic device parameters determining transport and recombination at the heterojunction interface. Fig. 1 shows an energy scheme of an a-Si:H(n)/c-Si(p) heterostructure. Key quantities for the performance of heterostructure solar cells are the electronic structure (band tails and defects) of the highly doped a-Si:H emitter layer, the a-Si:H/c-Si band offsets ΔE_C and ΔE_V, the interface state density $D_{it}(E)$ at the amorphous/crystalline interface, the built-in potential eV_D, and the minority carrier diffusion length in the Si-wafer.

In this survey we will present recent work performed at the Hahn-Meitner-Institut. In the first part we will discuss results from photoelectron spectroscopy which led to valuable information about the electronic structure of the heterojunctions and helped to optimize the device performance. In the second and third part we will discuss the properties and limitations of a-Si:H/c-Si heterojunctions as solar cells and light emitting diodes.

2. Electronic structure of a-Si:H/c-Si heterostructures

An adequate method for investigating the distribution of occupied states of the thin a-Si:H emitter layers with a thickness of 5 – 10 nm is photoelectron spectroscopy excited by near-ultraviolet light, NUV-PES [11,12]. An advantage of NUV-excitation with photon energies of 3 – 8 eV is a large electron escape depth of up to 10 nm due to the absence of surface or bulk plasmon generation, which would require higher energies of about 10 eV. In addition, the optical excitation probability is larger by several orders of magnitude for energies of 3 – 8 eV than for X-ray energies, which is the reason for a much higher sensitivity.

The results shown here were obtained in the constant final state yield spectroscopy mode, CFSYS, where the internal yield Y_{int} of the emitted photoelectrons was measured by varying the photon energy while keeping the detection energy constant. From $Y_{int}(E_{kin}, \hbar\omega) \propto N_{occ}(E_{kin} - \hbar\omega)$ the valence band edge, E_V, was determined from a fit of a model density of states distribution (DOS), broadened by the system response function (experimental resolution), to the experimental $Y_{int}(E_{kin}, \hbar\omega)$. Absolute values of the density of occupied states $N_{occ}(E)$ were obtained by normalizing Y_{int} at the valence band edge to a value of $N_{occ}(E_V) = 2 \times 10^{21}$ cm^{-3} eV^{-1}, which appears to be a reasonable value at the mobility edge [13]. Due to the limited photon penetration and electron escape depths, the measured distribution is a weighted average of the DOS of the sample up to a depth of 7 – 10 nm. The position of the Fermi level on the excitation energy scale can be determined from measurements on freshly evaporated Au films. Using this calibration, the position of the Fermi level in the thin a-Si:H layers can be determined.

For solar cells, the main function of the highly doped amorphous emitter is to build up a high band bending in the crystalline base of the heterojunction. Thus, it is necessary to control the position of the Fermi level in the amorphous layer by doping. Two main factors are conceivable that might diminish or completely prevent doping in ultrathin layers on conductive substrates: (1) The (oppositely doped) substrate might cause depletion of the layer from charge carriers. (2) There is evidence that the first nanometers as well as the interface region to the substrate of thick a-Si:H layers have higher densities of defects in the band gap than the bulk of the material. One therefore might expect that ultrathin layers of only a few monolayers entirely consist of such defect-rich material, which could lead to pinning of the Fermi level E_F. However, Fig. 2 shows that it is possible to dope 10 nm thin a-Si:H layers similarly as µm-thick films: The position of E_F relative to the valence band edge E_V can be varied from 0.55 eV for the boron doped to 1.04 eV for the intrinsic (not intentionally doped) and to 1.49 eV for the phosphorus doped film.

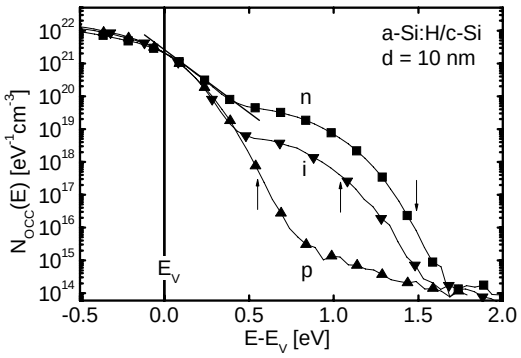

Fig. 2. Density of occupied states $N_{occ}(E)$ measured by CFSYS for differently doped a-Si:H films of 10 nm thickness deposited at 210 °C on crystalline silicon. Doping level: (■) 10^4 vppm P, (▼) undoped, (▲) 10^4 vppm B. The arrows mark the positions of the Fermi levels E_F. a-Si:H(n) and a-Si:H(i) were deposited on c-Si(p), a-Si:H(p) on c-Si(n). Reprinted from [12].

The DOS in Fig. 2 has the well known shape, consisting of the band of extended states at E < 0 eV, a valence band tail at 0 < E < 0.4 – 0.5 eV which decays exponentially into the band gap, and a Gaussian-like distribution of dangling bond defect states located deep in the band gap. For p-type a-Si:H, the dangling bond states are unoccupied and thus not accessible to photoelectron spectroscopy. The Urbach energies E_{0V}, defined by the slope of the exponential valence band tail, of ultrathin films are higher than those measured on thick device grade films with the same doping level: 61 meV for a-Si:H(i), 69 meV for a-Si:H(p), and 106 meV for a-Si:H(n). Also the densities of deep defects are much higher than commonly observed in thick films by photothermal deflection (PDS) or photocurrent spectroscopy (CPM): The integrated defect density amounts to $N_D = 2.9 \times 10^{18}$ cm^{-3} for the undoped film and reaches a value as high as 2.3×10^{19} cm^{-3} for the phosphorus doped

a-Si:H. It is most remarkable that for these thin a-Si:H films there is no correlation of N_D with the value of the Urbach energy. Such a correlation was observed for thick films and was interpreted as arising from an equilibration process between strained bonds in the band tail and dangling bonds in the deep defect band [14]. The different behavior of the thin films leads us to suppose that in ultrathin films, dangling bonds and deep defects are not in equilibrium. A detailed study of the dependence of N_D on the film thickness [15] led to the suggestion that growth-induced surface defects are annealed during growth until the strained bond-dangling bond system reaches its equilibrium. For the ultrathin films the defect structure probably cannot reach the equilibrium state with low defect density due to the very short deposition time of about 1 min.

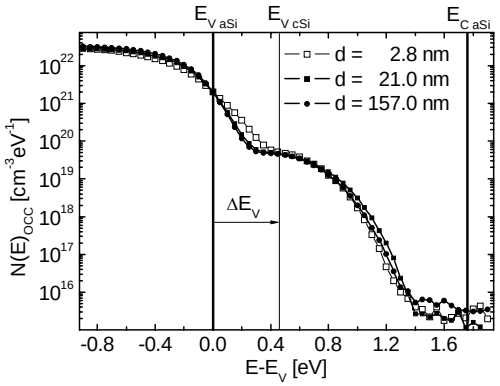

Fig. 3. $N_{occ}(E)$ of nominally undoped a-Si:H films on c-Si(p) measured by CFSYS. Deposition temperature 170 °C. Thickness: (□) 2.8 nm, (■) 21.0 nm, (●) 157.0 nm. Reprinted from [12].

A basic parameter of the a-Si:H/c-Si heterojunction is the alignment of the band gaps at the interface. There has been much uncertainty about the values of the band offsets ΔE_C and ΔE_V as determined from electrical measurements. The most direct way to obtain reliable information on these energies is a study of photoelectron spectroscopy on films the thickness of which is smaller than the escape depth of the excited electrons. In this case one expects that the photoemission signal contains contributions from the valence bands of both a-Si:H and c-Si. Fig. 3 shows the result of such a study on a series of a-Si:H/c-Si samples of different a-Si:H thickness. Whereas the curves of the two thicker films coincide, there is clearly an additional contribution in the signal of the thinnest sample (2.8 nm) at $E\text{-}E_V < 0.45$ eV which suggests that in this energy range, the signal is composed of contributions from the exponential edge in a-Si:H and the crystalline Si valence band. This behavior allows the exact determination of the valence band offset between a-Si:H(n) and c-Si(p,<111>) which gives a value of $\Delta E_V = 0.46 \pm 0.05$ eV. The conduction band offset of $\Delta E_C = 0.18 \pm 0.07$ eV then follows from the value of the a-Si:H band gap of 1.76±0.05 eV, which was determined from a Tauc plot of the spectral dependence of the photoconductivity of 300 nm thick a-Si:H layers. This asymmetrical alignment of the energy bands is a characteristic feature of the a-Si:H/c-Si heterojunction.

3. Heterojunction solar cells

In a-Si:H/c-Si heterojuntion solar cells the electronically active part is almost entirely the Si-wafer, the diffusion length of which is a decisive parameter for high efficiency. The challenge is to keep the density of defects in a-Si:H and the density of interface states as low as possible to prevent recombination losses. Particularly interesting are cell structures which use a-Si:H both as emitter at the front side and as passivating layer on the rear side of the Si-wafer. Fig. 4 shows the cell design used in our laboratory [9]. The cell structure consists, for instance, of n-type Si-wafers textured on both sides for better light absorption, the phosphorus doped a-Si:H (p) emitter layer covered by a transparent conductor (ZnO) and a highly boron doped a-Si:H(n) rear layer covered by an aluminum contact. Alternatively, the inverse doping sequence has been used. PECVD deposition offers the intrinsic advantage that the presence of atomic hydrogen in the plasma causes excellent passivation of the interface between the a-Si:H film and the crystalline Si substrate. Surface recombination velocities as low as 4 cm/s were reported for an a-Si:H(i) passivated Si surface [16]. The most sucessful approach so far is that of Sanyo Corp. [7] which involves a double heterostructure on an n-type Si-wafer: a-Si:H(p,i)/c-Si(n)/a-Si:H(i,n). It is a characteristic of this cell structure that thin buffer layers of undoped a-Si:H are used. In the last years several groups, particularly in Europe, have been working with the opposite doping sequence starting from p-type Si wafers. Applying traditional high temperature processing for the rear side (back surface field), conversion efficiencies of up to 17 % have been reported [8].

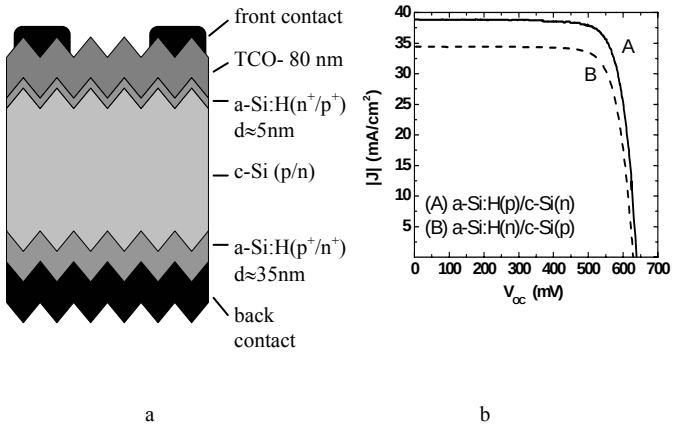

Fig. 4. (a) Scheme of a heterostructure solar cell (see text) and (b) I-V characteristics for the best cells with the different doping sequences under AM 1.5 illumination [9]. Area: 1 cm². Sample A: j_{SC} = 39.26 mA/cm², V_{OC} = 639.4 mV, FF = 78.9 %, η = 19.8 %; sample B: 34,9 mA/cm², 629 mV, 79 %, 17.4 %. Results confirmed at ISE Freiburg.

In view of the Sanyo results, an interesting question has been as to whether there are intrinsic advantages in the use of n-type Si wafers. We have addressed this question in a numerical simulation study where we calculated the solar cell efficiency as a function of the band offset and the density of states at the interface D_{it} (Fig. 5). The used simulation program AFORS-HET has been developed specifically for the study of such heterojunction solar cells [17, 18].

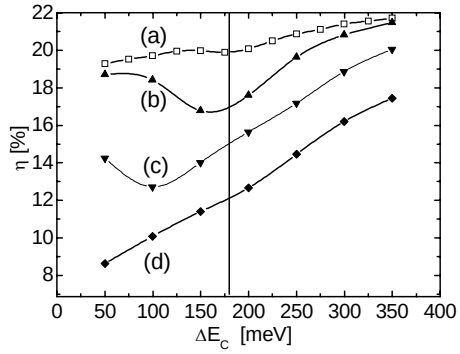

Fig. 5. Solar cell efficiency η versus band offset in the minority carrier band ΔE_C of c-Si for a-Si:H(n)/c-Si(p) [19]. Parameter is the interface state density D_{it}: (a) ≤ 1.0×10^{10} cm^2/eV, (b) 4.6×10^{10} cm^2/eV, (c) 2.2×10^{11} cm^2/eV, (d) 1.0×10^{12} cm^2/eV. The line marks the conduction band offset ΔE_C = 0.17 eV.

It turned out that both the band offset in the minority carrier band and the D_{it} are important parameters determining the performance of the solar cell. For the p-type Si-wafer the efficiency clearly increases with increasing value of the band offset in the conduction band ΔE_C and decreases strongly with increasing D_{it} (Fig. 5). The reason for this behavior is that recombination is suppressed when due to a large band offset in the minority carrier band of c-Si the concentration of recombining carriers at the interface is kept low. In case of the n-type c-Si wafer the minority carrier band is the valence band. This suggests that due to the large band offset of 0.45 eV at the valence band there may be an intrinsic advantage in the use of n-type Si wafers. The a-Si:H(p)/c-Si(n) interface may be less sensitive to recombination via interface states than the opposite doping sequence.

The solar cell structures shown in Fig. 4(a) were prepared applying the following procedure: a-Si:H was deposited by conventional plasma enhanced chemical vapor deposition (PECVD) at temperatures of 210 °C on float-zone grown crystalline Si-wafers (n- or p-type, 1-2 Ωcm, thickness 200 μm). Prior to the deposition of the a-Si:H layers, the wafers were treated by a standard RCA cleaning, conventional KOH/IPA pyramid etching and RCA cleaning sequences followed by an HF dip. A major challenge is the passivation of the textured Si surface. Separate measurements on Si-wafers showed that a sequence of wet chemical processes can reduce the density of recombination active surface states to a level as low as that of untextured wafers [9]. Measurements of the surface photovoltage decay on textured a-Si:H/c-Si structures revealed that this very sophisticated pretreatment also results in a reduction of the interface recombination in the solar cell structure after the a-Si:H deposition [19]. It is important to note that here no intrinsic buffer of a-Si:H(i) was used for passivation on either side of the device.

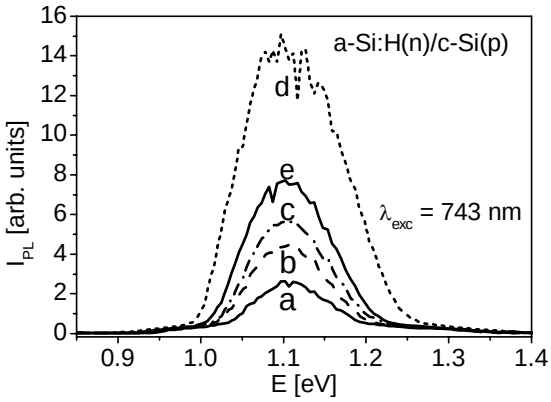

Fig. 6. Photoluminescence spectra of a-Si:H(n)/c-Si(p) structures prepared at different substrate temperatures [19]. (a) 65 °C, (b) 100 °C, (c) 140 °C, (d) 210 °C, (e) 300 °C.

The actual electronic structure and the recombination properties of the interface apparently are influenced by both the surface treatment prior to the deposition and the choice of the deposition parameters. As an example, Fig. 6 displays results of a study of photoluminescence on a set of a-Si:H(n)/c-Si(p) samples prepared at various deposition temperatures. The samples were illuminated by a laser pulse (743 nm) which is absorbed in the c-Si-wafer. The excited electrons and holes recombine radiatively in the bulk of the Si-wafer or non-radiatively at bulk defects and at the a-Si:H/c-Si interface. The integrated intrinsic photoluminescence intensity from c-Si was measured at 300 K. The photoluminescence intensity therefore is a direct measure of the electronic quality of the Si-wafer and the a-Si:H/c-Si interface. The spectra displayed in Fig. 6 clearly show that the emission depends on the a-Si:H deposition temperature and that the optimum temperature is at about 210 °C. Possibly this temperature leads to an optimum of the H-passivation and therefore optimized interface properties. However, it was also found that the defect structure of the a-Si:H film has pronounced influence on the recombination at the interface, for instance by offering additional tunneling recombination paths. The results from photoelectron spectroscopy also suggest an optimum substrate temperature of 210 °C. At this temperature the lowest values of the Urbach energy have been obtained.

Fig. 4(b) compares I-V characteristics of the two cell types. These solar cells were produced with optimized doping in the emitter layers of 2000 ppm P or B and a doping level in the passivating a-Si:H layer at the rear contact of 10^4 ppm. It has to be emphasized again that in contrast to the Sanyo approach, no intrinsic buffer layers have been used. A particularly important parameter is the thickness of the emitter layer. This layer should be as thin as possible in order to avoid absorption losses. However, it

should be thick enough to avoid depletion of charge carriers. Experimental results [17] and simulation studies [18] suggest an optimum thickness of 5 – 10 nm. The efficiencies obtained for the best cells of size 1 cm^2 amount to 17.4 % on c-Si(p) and 19.8 % on c-Si(n) substrates. These results have been confirmed independently at CalLab ISE Freiburg. As expected from the result in Fig. 5, the efficiency is considerably higher for the n-type Si wafer due to the large value of ΔE_V.

4. Light emitting diodes

Despite the indirect energy gap, silicon pn-junction solar cells exhibit band-edge emission under forward bias. For the best solar cells ($\eta > 21$ %) with improved light trapping structures and very effective reduction of non-radiative recombination in the bulk and at the cell surfaces, an external light emission efficiency of close to 1 % has been reported [20]. The emission occurs at the silicon band edge and is described by Planck's law, modified by the absorbance of the material. A simpler and perhaps more easily producible scheme for a Si-LED is the a-Si:H/c-Si heterostructure which so far shows emission efficiencies of up to 0.3 % [10]. The results that will be discussed here were obtained on solar cells of ZnO/a-Si:H(n)/c-Si(p) prepared on Fz-Si wafers as described in [8]. Two types of devices with an area of A = 1 cm^2 are compared: (A) textured Fz-Si(Al), 8 nm emitter, and 35 nm a-Si:H(p)/Al back contact; (B) flat Fz-Si(B), 20 nm emitter, and boron-diffused/Al back contact. The electrical characterization at 300 K under AM 1.5 illumination led to the following results for short circuit current densities j_{SC}, open circuit voltages V_{OC}, fill factors FF and solar efficiencies η: (A) 34.1 mA/cm^2, 610 mV, 79.9 %, 16.6 % and (B) 28.9 mA/cm^2, 638 mV, 77 %, 14.2%.

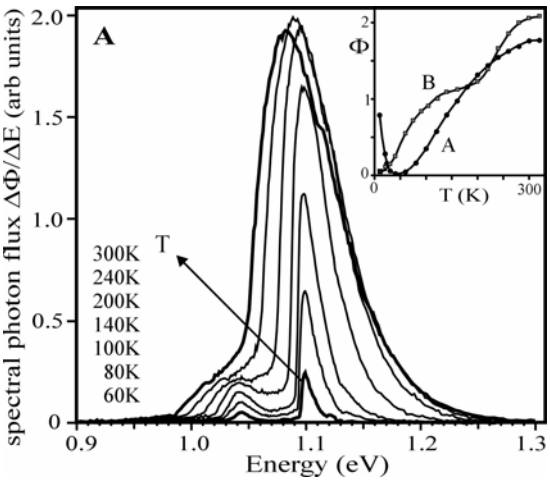

Fig. 7. Electroluminescence spectra of sample A, recorded at a forward bias current density j_f of 50 mA/cm^2 at various temperatures. Reprinted from [10].

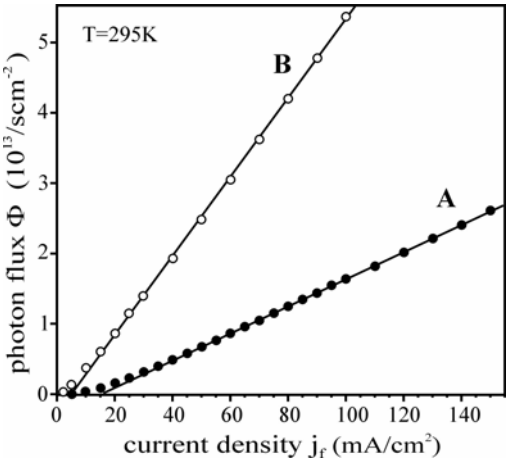

Fig. 8. Total emitted flux Φ as a function of the current density for samples A and B. Reprinted from [10].

Above 50 K the shapes of the electroluminescence and photoluminescence spectra were identical for all samples. Fig. 7 displays electroluminescence spectra of sample A which were recorded at various temperatures using a cooled Ge detector and lock-in technique. The spectra are dominated by intrinsic radiative recombination of electron-hole pairs in the c-Si wafer with simultaneous creation of TO phonons. At lower temperatures more finestructure appears which can be attributed to emission of a TA phonon and two-phonon transitions involving Umklapp processes. The integrated intensity increases with temperature for both samples (insert in Fig. 7). The total emitted photon flux Φ measured in an integrating sphere increases linearly with the current density for both samples (Fig. 8). The slope is related to the external quantum efficiency. The power efficiency defined by the ratio of the emitted light power and the consumed electrical power reaches values of 0.32 % (sample B) and 0.14 % (sample A). Despite of a higher conversion efficiency as a solar cell, the emission efficiency of the textured sample A is smaller than for the untextured sample B. This observation is consistent with the fact that sample B has a higher open circuit voltage V_{OC}. Obviously, in the present case texturization enhances the short circuit current density j_{SC} by an improvement of optical absorption but causes a decrease of V_{OC}, probably due to the enhancement of the density of interface states of the rough Si surface. Yet texturization results in a higher conversion efficiency. Both V_{OC} and the emission intensity are determined by the splitting of the quasi Fermi levels which is identical with the chemical potential of the electron-hole pairs. Therefore, high emission intensity should be related to a high value of V_{OC}.

According to the results in Fig. 7, the emitted photon flux, Φ, increases with temperature. Such behavior is rather unexpected. The theoretical analysis [10] starting from the generalized Planck equation suggested that for an ideal diode, Φ should rather decrease with increasing temperature. Numerical simulations revealed that the observed behavior may arise from the influence of interface states. The simulations were performed using the

program AFORS-HET which allows to calculate observables of heterojunction solar cells from internal device parameters. The present simulation used a standard parameter set [17,18] for an untextured device structure of 10 nm a-Si:H(n)/interface/300 µm c-Si(p). The interface was modeled by an energy-independent distribution of interface states, D_{it}.

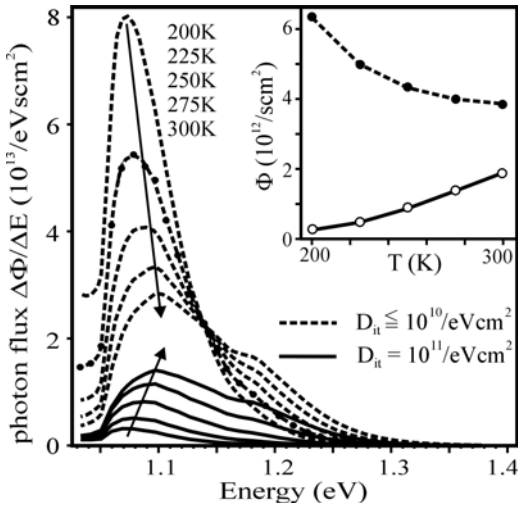

Fig. 9. Numerical simulation of the emission spectra at various temperatures and two values of the interface state density $D_{it.}$ Reprinted from [10].

The electroluminescence spectra were calculated from the generalized Planck equation using standard absorption spectra of a-Si:H(n) and c-Si and inserting as chemical potential of the electron-hole pairs the splitting of the quasi Fermi levels. The result of such simulations is displayed in Fig. 9 which shows electrolumincence spectra calculated for a current density of 30 mA/cm^2 at various temperatures for two values of the interface state density D_{it}. These results are interesting mainly for two reasons:

(1) The shape of the calculated spectra deviates in some aspects from the experimental spectra in Fig. 7. There is the dominating band at $\hbar\omega < E_G$ (≈1.15 eV) due to recombination of e-h pairs with emission of phonons and an additional shoulder for $\hbar\omega > E_G$ due to photon emission with annihilation of TO-phonons which is not observed in the experiment. The detailed discussion of these differences [21] resulted in the suggestion that due to their different dynamics, the photon and phonon systems cannot reach equilibrium such that the assumption of equilibrium in Planck's equation overestimates light emission with the simultaneous annihilation of a phonon at $\hbar\omega > E_G$.

(2) The other interesting aspect concerns the influence of interface states on the temperature dependence of the emission. For low values of D_{it} ($\leq 10^{10}$ eV^{-1}cm^{-2}) there is negligible influence of recombination on the chemical potential and the temperature dependence is as expected from theory: The emission intensity at energies above the band gap ($\hbar\omega > E_G$) increases with increasing temperature, while the intensity for $\hbar\omega < E_G$ decreases. The crossover of these two contributions marks the c-Si band gap E_G (1.15 eV). As a result, the integrated emission decreases as shown in the inset of the figure. At higher values of D_{it}, the behavior changes significantly: For $D_{it} = 10^{11}$ eV^{-1}cm^{-2} the intensity is reduced in the entire range since interface recombination reduces the chemical potential and, more importantly, the temperature dependence is reversed. As interface recombination is more efficient at low temperatures, light emission increases with temperature.

5. Final remarks

a-Si:H/c-Si heterojunctions offer a very interesting approach for a simple and less expensive solar cell technology. These solar cells have been shown to be efficient light emitters when operated as light emitting diode. High solar cell efficiencies of 21.8 % have been obtained on Si-wafers in the laboratory using intrinsic a-Si:H(i) buffer layers [7] and module fabrication based on this HIT technology has been started. But also without such buffer layers, efficiencies as high as 19.8 % have been reported [9]. This technology offers the advantage that it combines wafer technology with thin-film techniques which are capable of large area deposition and allow low process temperatures. Therefore, this technique is not only interesting as an approach for very high efficiencies on monocrystalline Si wafers. Heterojunctions instead of diffused junctions can also become an attractive concept when low-cost Si absorbers are used which may require low-temperature processing. At present, research is pursued which aims at applying the heterojunction concept to realize a polycrystalline Si thin film solar cell processed at temperatures below 500 °C on foreign substrates [22].

Acknowledgement

This article is dedicated to Professor Radu Grigorovici, whom we owe outstanding contributions to the field of amorphous semiconductors, on occasion of his 95th birthday. W. F. is grateful for many inspiring and encouraging conversations.

References

[1] R. Grigorovici, N. Croitoriu, A. Devenyi, E. Teleman, Proc. VII Int. Conf. Phys. of Semiconductors (Dunod, Paris) 423 (1964).
[2] R. Grigorovici, N. Croitoriu, M. Marina, L. Nastase, Rev. Roum. Phys. **13**, 317 (1968).
[3] R. C. Chittik, J. H. Alexander, H. F. Sterling, J. Electrochem. Soc. **116**, 77 (1969).
[4] R. J. Loveland, W. E. Spear, A. Al-Sharbaty, J. Non-Cryst. Solids **13**, 55 (1973).
[5] W. Fuhs, K. Niemann, J. Stuke, AIP Conf. Proceed. **20**, 345 (1974).
[6] T. Sawada, N. Terada, S. Tsuge, T. Baba, T. Takahama, K. Wakisada, S. Tsuda, S. Nakano, Proc. 1st World Congress on Photovoltaic Energy Conversion (Hawaii) 1219 (1994).
[7] M. Taguchi, H. Sakata, Y. Yoshimine, E. Maruyama,

A. Terakawa, M. Tanaka, Proc. 31st World Congress on Photovoltaic Energy Conversion (Lake Buena Vista) 866 (2005).
[8] See survey: K. V. Maydell, E. Conrad, M. Schmidt, Prog. Photovolt: Res. Appl. **14**, 289 (2006)
[9] E. Conrad, K. V. Maydel, H. Angermann, C. Schubert, M. Schmidt, Proc. 4th World Congress on Photovoltaic Energy Conversion (Waikoloa, USA) in print (2006).
[10] W. Fuhs, A. Laades, K. V. Maydel, R. Stangl, O. B. Gusev, E. I. Terukov, S. Kazitsyna-Baranovski, G. Weiser, J. Non-Cryst. Solids **352**, 1884 (2006).
[11] K. Winer, L. Ley, Phys. Rev. B **36**, 6072 (1987).
[12] M. Schmidt, A. Schoepke, L. Korte, O. Milch, W. Fuhs, J. of Non-Cryst. Solids **338 - 344**, 211 (2004).
[13] R. A. Street, Hydrogenated Amorphous Silicon, Cambridge University Press, Cambridge, 1991.
[14] M. Stutzmann, Phil. Mag. B **60**, 531 (1989).
[15] N. Hata, S. Wagner, P. Roca i Cabarrocas, M. Favre, Appl. Phys. Lett. **56**, 2448 (1990).
[16] S. Dauwe, J. Schmidt, R. Hetzel, Proc. 29th Photovoltaic Specialists Conference (IEEE), 1246 (2002).
[17] R. Stangl, A. Froitzheim, M. Schmidt, W. Fuhs, Proc. 3rd World Conf. on Photovoltaic Energy Conversion (Osaka, Japan) 4P-A8-45 (2003).
[18] R. Stangl, M. Kriegel, K. V. Maydell, L. Korte, M. Schmidt, W. Fuhs, Proc. 31st IEEE Photovoltaics Specialists Conference (IEEE) 1556 (2005).
[19] M. Schmidt, L. Korte, A. Laades, R. Stangl, Ch. Schubert, H. Angermann, E. Conrad, K. V. Maydell, Thin Solid Films, submitted (2006).
[20] M. Green, J. Zhao, A. Wang, P. J. Reece, M. Gal, Nature **412**, 805 (2001),
[21] G. Weiser, S. Kazitsyna-Baranovski, R. Stangl, Proc. ICOOPMA 2006.
[22] W. Fuhs, S. Gall, B. Rau, M. Schmidt, J. Schneider, Solar Energy **77**, 961 (2004).

*Corresponding author: fuhs@hmi.de